Astronomy & Astrophysics manuscript no. output
April 2, 2020

The future of IMF studies with the ELT and MICADO

The local Universe as a resolved IMF laboratory

K. Leschinski[1] and J. Alves[1]

Department of Astrophysics, University of Vienna, Vienna, Austria
e-mail: kieran.leschinski@univie.ac.at

Received TBD; accepted TBD

ABSTRACT

Context. Young stellar clusters in the local Universe provide the most pristine information on the stellar Initial Mass Function (IMF), but their stellar densities are too high to be resolved by present-day instrumentation. With a resolving power 100 times better than the Hubble Space Telescope, the MICADO near-infrared camera on the Extremely Large Telescope (ELT) will provide access for the first time to a significant number of dense young stellar clusters critical to direct studies on the universality and shape of the IMF.
Aims. In this work we aim to estimate the lowest stellar mass that MICADO will be able to robustly detect given a stellar density and distance.
Methods. We used SimCADO, the instrument simulator package for the MICADO camera, to generate observations of 42 dense stellar regions with densities similar to the cores of young stellar clusters. The densities of these stellar fields ranged from 10^2 to 10^5 stars arcsec^{-2} , and the fields were placed at distances from 8 kpc to 5 Mpc from the Earth. The lowest reliably observable mass for each stellar field was determined via PSF subtraction photometry.
Results. Our results show that true **TRUE? WHAT DO YOU MEAN?** stellar densities of $<10^3$ stars arcsec^{-2} will be easily resolvable by MICADO. The lowest reliably observable mass in the LMC will be around 0.1 $M_\odot$ for clusters with densities $<10^3$ stars arcsec^{-2} . MICADO will unlock the stellar content of the cores of all dense young stellar clusters in the Magellanic clouds, allowing the peak and shape of the IMF to be studied in detail outside the Milky Way. At a distance of 2 Mpc all stars with $M > 2\,M_\odot$ will be resolved in fields of $<10^4$ stars arcsec^{-2} , allowing the high-mass end of the IMF to be studied in e.g. NGC 300.
Conclusions. We show that MICADO on the ELT will be able to access star clusters 10× denser than what JWST will be able to access, and over 100× denser than those imaged by Hubble. While the sensitivity of MICADO will not allow us to study the brown dwarf regime outside the Milky Way, it will allow access to all the members (stellar and sub-stellar) of the densest star clusters in the Milky Way and all stellar members in the Magellanic clouds clusters, allowing for a giant step for resolved IMF research (OR SOMETHING LIKE THE YOUR SUMMARY SENTENCE. **HOW MANY CLUSTERS ARE THERE IN THE SMC/LMC?**

1. Introduction

The stellar Initial Mass Function (IMF), or the spectrum of stellar masses at birth, has implications in almost all fields of astrophysics. On the local scale, the IMF determines the fate of a star formation region and determines the environment that emergent planet-forming circumstellar disks will be exposed too. On the large scale, the IMF is irrevocably connected to the composition of the stellar populations in a galaxy and has a massive impact on the mass and energy cycle of a galaxy. For example, the larger the amount of mass locked up in low mass stars, the smaller the reservoir of gas for the next generation of stars and the smaller the enrichment of the interstellar medium (ISM). Finally, cosmological simulations of galaxy formation and galaxy clusters inevitably rely on an universal the IMF to determine stellar yields and the strength of feedback mechanisms governing the transport of energy and material. In short, the IMF is a fundamental parameter in astronomy.

In his original work, Salpeter (1955) used a single power-law distribution with a slope of 2.35 to describe the IMF for masses between ∼1 and ∼10 $M_\odot$. This description was later modified to a series of broken power laws to include the stars below the hydrogen-burning limit by Kroupa (2001). Chabrier (2005) proposed a log-normal distribution with a power-law modification for the high and low mass regions. Although not an important goal per se as both descriptions are empirical and not the prediction of a theory, it has proved difficult from observations to decide which of these two descriptions more aptly describes the IMF because they are similar.

Most observational studies suggest that the shape of the IMF is constant (Kroupa 2002; Bastian et al. 2010). Solid deviations from the accepted IMF form are elusive, and at the moment, often controversial. Still, there is one major aspect that hinders general acceptance of a universally constant IMF: a lack of directly derived IMF (star counts) for environments substantially different from the solar neighbourhood. Table 1 shows that even in the closest star forming galaxies like the large and small Magellanic clouds, only the Hubble space telescope (HST) has the sensitivity to reach below one solar mass (See references in Table 1). Long exposures with HST have observed stars just below the first break in the Kroupa power law at 0.5 $M_\odot$ (Da Rio et al. 2009; Kalirai et al. 2013; Geha et al. 2013), but not far enough into the lower mass regions to put constraints on the shape of the IMF in these extragalactic environments. Adding to observers' woes is the lack of spatial resolution. At the distance of the LMC, star forming regions can contain anywhere from 10^2 to 10^5 stars arcsec^{-2} . A perfect example of why current studies struggle to reliably determine the IMF for dense stellar populations outside the Milky Way is given in Figure 1 of Sirianni et al. (2000). The picture shows a cluster core (R136) being completely dominated by the flux of the brightest stars. Thus studies of the IMF are limited to the outer regions of these clusters where stellar densi-

Table 1. A compilation of mass limits for a selection of studies of the IMF outside the Milky Way with the Hubble space telescope. It should be noted that for the study by Gallart et al. (1999) the estimated global star formation history was consistent with a Salpeter slope, rather than a Salpeter slope being extracted from the photometric data.

Galaxy	Target	Distance kpc	Mass range $M_\odot$	IMF Slope(s)	Break Mass $M_\odot$	Reference
LMC	R136	50	2.8-15	2.22		Hunter 1995
LMC	NGC 1818	50	0.85-9	2.23		Hunter 1997
LMC	R136	50	1.35-6.5	2.28, 1.27	2.1	Sirianni 2000
LMC	LH 95	50	0.43-20	2.05, 1.05	1.1	Da Rio 2009
SMC	NGC 330	62	1-7	2.3		Sirianni 2002
SMC	NGC 602	62	1-45	2.2		Schmalzl 2008
SMC		62	0.37–0.93	1.9		Kalirai 2013
Hercules		135	0.52-0.78	1.2		Geha 2013
Leo IV		156	0.54-0.77	1.3		Geha 2013
Leo I*		250	0.6-30	2.3		Gallart 1999

ties are low enough for individual low mass stars to be resolved. The age of a cluster and the resulting level of mass segregation can also skew the results when considering the IMF in massive clusters (Lim et al. 2013). However without being able to study the core of such clusters inside and outside the Milky Way, it is difficult to determine to what extent this plays a role. Thus in order to systematically study the lower mass, and arguably most interesting, part of the IMF telescopes with higher spatial resolution and better sensitivity than the current generation of ground and space based telescope will be needed.

In the middle of the next decade, the era of the extremely large telescopes will begin. ESO's Extremely Large Telescope (ELT) (Gilmozzi & Spyromilio 2007) with the help of advanced adaptive optics (Diolaiti 2010) will offer the power to resolve spatial scales at the diffraction limit of a 40m-class mirror. This will provide an improvement of a factor of ~15× over HST and a factor of ~6× over the future JWST telescope. With a collecting area of 978 m^2 the ELT will have at least the same sensitivity as the HST in sparse field and will be able to observe much deeper than HST in crowded fields. The MICADO instrument (Davies et al. 2010, 2016) will be the ELT's first-light near-infrared (NIR) wide-field imager and long slit spectrograph. With a plate scale of 4 mas and an AO corrected field of view of almost a square arcminute, MICADO aims to address exactly this niche.

The main focus of this paper is to determine to what extent MICADO will improve our ability to study the IMF and other properties of dense stellar populations is the main focus of this paper. In this paper we have attempted to addressed the following two questions: What is the lowest mass star that MICADO will be able to observe for a given density and distance? What instrumental effects will play a critical role when undertaking such studies with MICADO and the ELT? In our quest for answers we used SimCADO, the instrument data simulator for MICADO (Leschinski et al. 2016), to simulate a wide range of densely populated stellar fields at various distances, which can act as cluster proxies. The current version of SimCADO takes into account all the major and most of the minor spatial and spectral effects along the line of sight between the source and the detector. We used the software to generate realistic images of our model stellar fields and then conducted several iterations of PSF photometry and star subtraction to extract as many stars as possible from the simulated observations. The extracted stars were compared with the input catalogue to determine the completeness of the extraction and to define a "limiting reliably observable mass" for the different stellar field densities and distances.

This paper is organised in the following way: Section 2 describes the stellar fields used in our simulations and how the simulations were run. In this section we also describe the algorithm for detecting and subtracting stars in the simulated images. In Section 3 we describe the results of the simulations and discuss their validity in the context of possible future observations of real young stellar clusters. Section 4 summarises our results.

2. Data sets

The best way to determine the IMF is to look at a population of stars which is still young enough for all the original members to still be around, yet old enough that the main phase of star formation activity. If a population is too young, it will not have finished forming all its stars and dust extinction will be a major source of uncertainty and incompleteness. Too old and the most massive members will already have exploded as supernovae. Dynamical effects will also have led to evaporation of stars from the cluster. Unfortunately such ideal conditions are hardly met. Star formation happens on time scales of 10^6 years. The most massive stars burn their hydrogen reserves within the first several ten million years and move off the main sequence. Given that the dispersion time for stellar clusters is on the order of hundreds of millions of years, at any point in time relatively few of the observable new clusters will be so youthful. The majority of IMF studies focus on the clusters which come closest to meeting these conditions - namely open clusters (OC) and young massive clusters (YMC). It should be mentioned that OB associations also provide a laboratory for studying the IMF. However as these are older and in many cases more spread out, the chances of contamination from background sources and missing ejected stars is higher. Furthermore, the high mass end of the IMF cannot be observed as the highest mass stars have already left the main sequence, and some have ended as supernova.

2.1. Parameter Space

The HST has a diffraction limit of ~0.1" at 1.2 μm and can reach magnitudes of up to J=28.6^m (Rajan & et al. 2011) in a 10 hour observation. Using AO assisted ground based instruments like NACO at the VLT, diffraction limited observations can be achieved over small (~1') fields of view. The diffraction limit of the VLT telescopes is ~0.03" at 1.2 μm , 3× smaller than HST, however NACO only has a sensitivity limit of around J=24^m . As boundary conditions for our suite of stellar fields we took the resolution limit of HST, as cluster cores with densities lower than

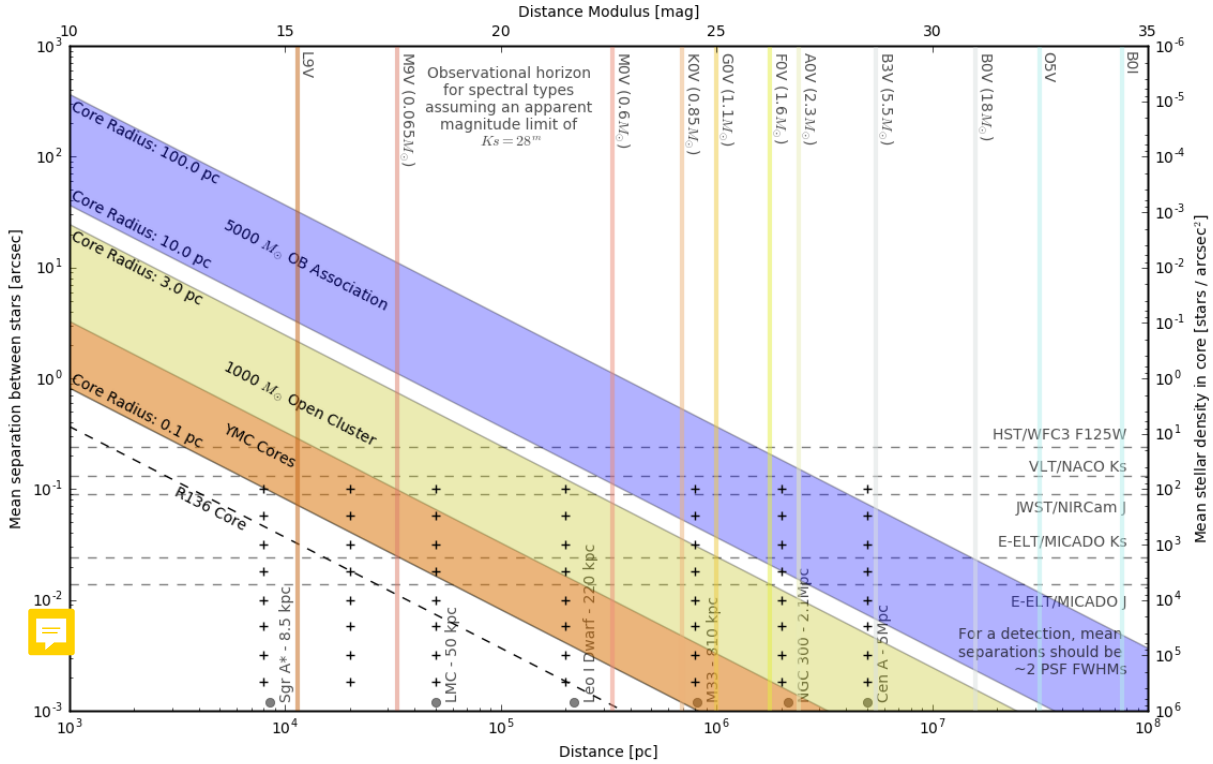

Fig. 1. The crosses represent the parameter space covered by the simulated stellar fields in this study relative to the estimated core stellar densities for the three major categories of young stellar populations: open clusters (green), young massive clusters (orange), and OB associations (blue). The vertical lines represent the furthest distance at which a certain type of main sequence star will still be above the detection limit of MICADO, i.e. Ks=28^m . The dashed horizontal lines show the theoretical confusion limit for MICADO, JST, HST and NACO/VLT. The confusion limit assumes an average minimum distance of 2× the PSF FWHM between stars. Obviously for NACO confusion would not play as much of a role as the instruments sensitivity limit is Ks~24^m .

this are already accessible to the HST. Assuming an average of one star per FWHM, our lower density limit was set to 100 stars arcsec^{-2} . To find the upper density limit we first took the theoretical diffraction limit of the ELT: 7 mas at 1.2 μm, or 2×10^4 stars arcsec^{-2} . However as faint stars drop below the telescope's detection limit the effective density of detectable stars decreases with increasing distance. As we wanted crowding limited observations at large distances (>1 Mpc), we increased the true stellar density by a factor of 15× so that the M > 1 $M_\odot$ stars alone would meet the crowding criterion. Thus we set the upper limit for the true stellar density to 3×10^5 stars arcsec^{-2} .

Current telescopes are capable of detecting almost all main sequence stars above the hydrogen burning limit (~0.08 $M_\odot$) within a few kiloparsecs of the Sun. Detecting all main sequence stars in clusters which are further a field, e.g. in the galactic centre and beyond, is where MICADO's increased sensitivity and resolution will bring the greatest breakthroughs. Indeed the question of whether the IMF is truly universal dictates that we study the IMF outside the Milky Way. Therefore we placed our model proxy-clusters at distances corresponding to some of the more well known celestial landmarks: The Galactic Centre (~8 kpc), the LMC (~50 kpc), Leo I dwarf galaxy (~200 kpc), M33 (~800 kpc)[1], NGC 300 (~2 Mpc), and Cen A (~5 Mpc). Figure 1 shows the parameter space covered by average (~1000 $M_\odot$) open clusters with radii between 0.1 pc and 3 pc and average OB Associations (~5000 $M_\odot$) with radii between 10 pc and 100 pc as distance from Earth increases. The lower bounds of the open cluster parameter space also covers the cores of YMCs. Average cluster properties were derived for the OB Associations from Mel'Nik & Efremov (1995), for the open clusters from Piskunov et al. (2007), and for the YMCs from Portegies Zwart et al. (2010).

2.2. Artificial stellar fields

In this study we generated densely populated stellar fields, that could function as proxies for the dense regions at the cores of young stellar clusters. The parameter space covered by these cluster proxies are shown with the crosses in Figure 1. The size of each stellar field was set at 2"×2" (See section 2.3). The stellar fields were populated by continually drawing stars from an IMF until the required stellar density was reached. The mass of each star was drawn at random from an IMF distribution with minimum and maximum masses of 0.01 $M_\odot$ and 300 $M_\odot$. The IMF followed a standard Kroupa (2001) broken power law distribution with breaks at 0.08 $M_\odot$ and 0.5 $M_\odot$ and standard slope expo-

[1] The author recognises that the location of the ELT in the southern hemisphere means that M33 will effectively be unobservable. We provide this data point because M33 will, with luck, be visible to the Thirty Meter Telescope.

nents[2]. The absolute J and Ks magnitudes for each star were calculated by interpolating Table 5 in Pecaut & Mamajek (2013)[3] for the given mass. The requisite distance modulus for the stellar fields was added to give each star an apparent magnitude. It should be noted that we did not include extinction in the distance modulus as this varies with the line of sight. The stars were assigned random coordinates within the 2 arcsec bounding box. Although true clusters follow some sort of luminosity profile, and hence density profile, for this study we were primarily interested in the densest regions, i.e. the worst case scenario. Hence distribution of stars in our stellar fields followed a uniform random distribution. In real observations the decline in density with radial distance will therefore be advantageous and offer an improvement over our pessimistic approach.

2.3. Observations

To "observe" our stellar fields we used the standard imaging mode of SimCADO (Leschinski et al. 2016) which mimicked observations with the wide-field mode of MICADO at the ELT. The core regions of open clusters and YMC have radii on the order of ∼1 pc (Portegies Zwart et al. 2010). At a distance of 200 kpc (∼Leo 1 Dwarf), this translates to an angular diameter of ∼2". Thus we thought it safe to assume that the stellar density within the inner 2"x2" region should remain relatively constant. For the sake of computational effort we decided to restrict to observations to this 2"x2" window in the centre of the detector.

At the very least multi-band photometry is required to determine the mass of a star. Therefore detections in at least the J and K_S filters is necessary. We deemed a detection in the K_S filter to be critical for any study of the IMF and therefore restricted our observations to this filter. The reason for this is as follows: The sky background in the K_S filter is the highest of all NIR filters and the stellar flux is for all main sequence stars (and many brown dwarfs) weakest in the K_S filter. If a source is undetectable in the K_S filter it will not be possible to determine its mass accurately. Given the AO-nature of the observations and the expected low Strehl ratio at 1.2μm (Clénet et al. 2016), it could be argued that defections in the J filter will be more difficult. In the end the fluxes of the stars and the sky are set by nature, whereas the Strehl ratio is a question of engineering and optical design. The stars cannot be made brighter, whereas optical quality can be improved. Hence we deemed a detection in the K_S filter to be the critical point for determining the mass of cluster members.

Exposure times were kept to 1 hour for no other reason than observing time at the ELT will be in very high demand once it comes on line and observations in two or more filters are needed to accurately determine the mass of stars.

2.4. Source extraction and matching

Figures A.1 and A.2 in the Appendix show a graphical representation of the process described in this section. They show two examples of "observed" stellar fields placed at a distance of 50 kpc and containing 10^3 and 10^4 stars arcsec^{-2} respectively. The stark features of the SCAO PSF[4] are clearly visible in the images. The diffraction core of the PSF is however still well modelled by a Gaussian distribution. To find and measure the stars in the images we used the following method:

1. Find the brightest star in the image with `DAOStarFinder` from `photutils` (Bradley et al. 2017)
2. Find the centre of the star in a 5×5 pixel window around the coordinates given by `DAOStarFinder`
3. Fit a 2D Gaussian profile to the core of the star
4. Scale an image of a reference star to match the amplitude, baseline and offset of the found star
5. Subtract the scaled reference star from the image
6. Repeat until `DAOStarFinder` no longer finds any sources above 5 σ

In practice we found that we could subtract ∼100 stars at once and thus greatly increase the speed of the process. The amplitudes and baselines were converted to magnitudes based on the reference star. Our reference star was a solitary "field" star with a magnitude of K_S=15, observed for the minimum MICADO exposure time of 2.6 s. We calculated masses for each star based on the observed fluxes in the K_S filter. This step is only permissible because of the simplified context of this study. We are free to equate the luminosity function with an equivalent mass function because all our stellar fields have the intrinsic property that they only contain main sequence stars and the luminosity and mass functions enjoy a one-to-one relationship for this conversion in the K_S filter, mathematically speaking. Furthermore, our primary goal is to determine what the lowest reliably observable mass is, based on how well MICADO will perform in crowded field - not to directly measure the mass of the original stars. We feel that this step does not detract from achieving the goal of this study.

Finally we cross-matched the coordinates of the extracted sources with the original table of coordinates to determine what fraction of stars were correctly detected with our algorithm. Due to noise and confusion from very close stars the centroid coordinates of the extracted star was not always exactly equal to the original coordinates. The cross-matching algorithm was instructed to search for the closest star within a 25 mas radius. If a fainter or brighter star happened to be closer, then the algorithm chose that star from the catalogue as the match. We determined whether the extracted masses for stars in a certain mass bin were "reliable" by binning the extracted stars according to mass. We then took the mean and standard deviation of all stars within a mass bin. As long as the mean extracted mass to true mass ratio was in the range 1.0±0.1 and the standard deviation was less than 0.1, the mass bin was classed as reliable. By this definition the lowest reliably detectable mass for a stellar field was given by the lower edge of the lowest mass bin which satisfied these criteria.

3. Results and Discussion

3.1. The lowest reliably observable masses for given stellar densities and distances.

The first of the questions we asked with this study – "What is the lowest mass star that MICADO will be able to observe reliably

[2] By "standard" we mean: $\alpha = 0.3$ for $M < 0.08M_\odot$, $\alpha = 1.3$ for $0.08M_\odot < M < 0.5M_\odot$, and $\alpha = 2.3$ for $M > 0.5M_\odot$ as defined in Kroupa (2001)

[3] Masses are actually not given in Table 5, but rather in the online suppliment at `http://www.pas.rochester.edu/~emamajek/EEM_dwarf_UBVIJHK_colors_Teff.txt`

[4] The PSF user here was from a simulation of the SCAO mode from MAORY. It was only released internally within the MAORY consortium. By default the SimCADO package comes with a SCAO PSF generated by the MICADO consortium, which is in the public domain.

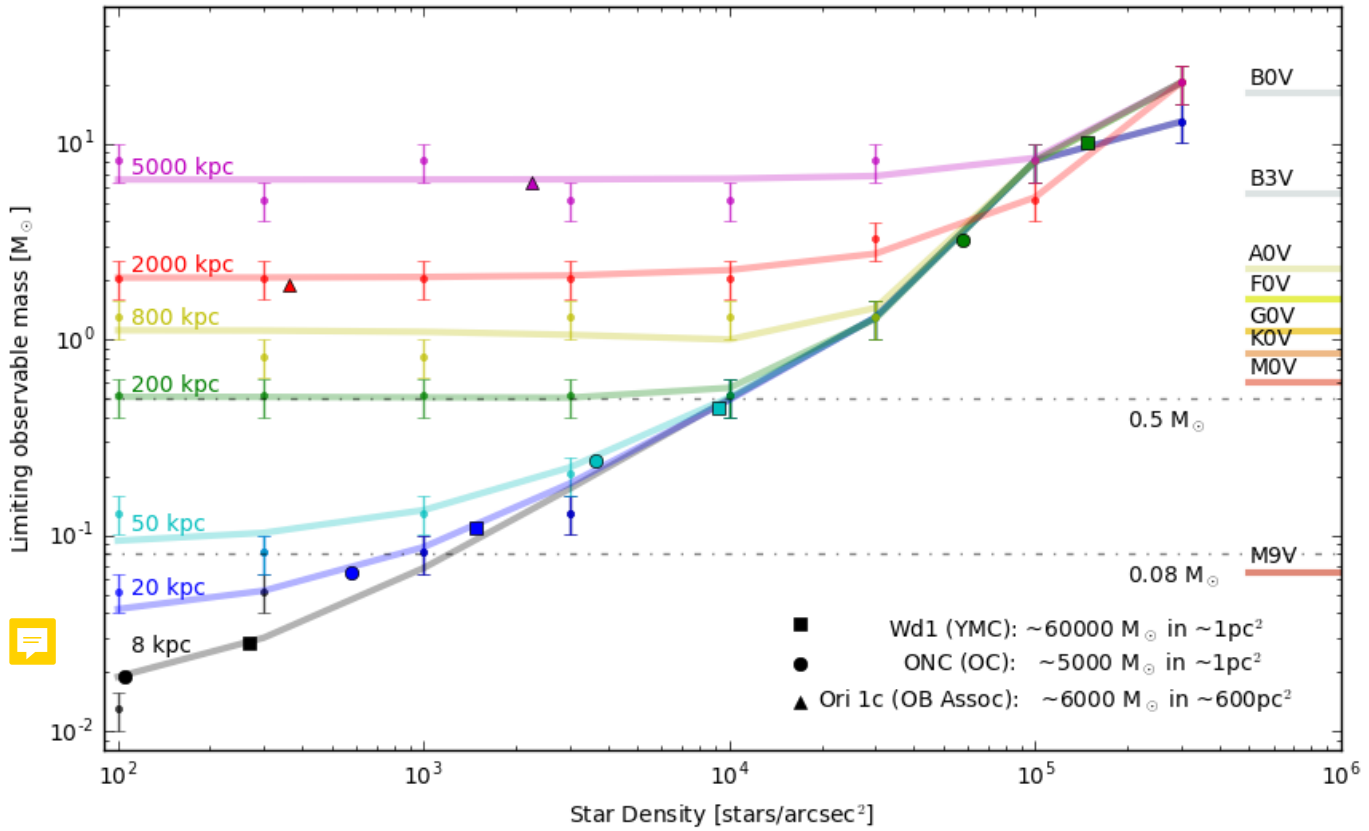

Fig. 2. This graph is the answer to the first question we posed: what is the lowest observable mass for given stellar densities and distances? The errors in the observable mass are 0.2 dex and correspond to the size of the mass bins used. Two trends are visible in the best fit lines for each distance: the flat regime shows that the limiting mass is based on the sensitivity limit of MICADO, while the exponential regime shows where crowding becomes the limiting factor. The cavity to the lower right shows the parameter space in which stars of a given mass will not be observable. Here the stellar density includes all the stars in a given area down to 0.01 $M_\odot$, not just the stars above the sensitivity limit. Hence for the cases where observations are sensitivity limited, the effective observable star density is, in the cases with greater distance, much lower. In these cases the stars below the sensitivity limit only contribute to a higher background flux.

for a given density and distance?" – can be answered by Figure 2. For each of the distances and densities we have plotted the lowest reliable mass bin. The scatter in the plot reflects the random nature of the simulations. The positions of the stars in each of the stellar field were randomised, the sampling of the mass function was random and detector and shot noise was applied to the image as part of SimCADO's read-out process. Thus no two stellar fields were the same. Each stellar field configuration was only run once. We therefore only have one data point for each density and distance. The bin size used for the reliability statistics was set to 0.2 dex, and is therefore the uncertainty in the limiting observable mass.

From Figure 2 we can immediately see the two limiting regimes of sensitivity and crowding. The flat parts of the curves in Figure 2 show the densities for which MICADO will be sensitivity limited at each distance and the diagonal regions show when crowding becomes the limiting factor. For example observations of a cluster at a distance of 8 kpc observations will always be crowding limited for densities above 100 stars arcsec^{-2}. At a distance of 200 kpc observations will be limited by sensitivity up to a density of 10^4 stars arcsec^{-2} , thereafter crowding will be the dominant factor. At 5 Mpc all observations will be sensitivity limited. As a reference we have included the approximate stellar densities for three well known young clusters in Figure 2 *if they were located at the distance of the simulated clusters.* For example, if the YMC Westerlund 1 were to be located in the LMC, it would fall in to the crowding-limited regime for MICADO. The lowest reliably observable mass in the densest region of the core would only be ~0.5 $M_\odot$. This is equivalent to what HST is capable of observing in the outer rim territories of LMC clusters. For clusters in the LMC with stellar densities less than 10^3 MICADO will be limited by sensitivity to masses above 0.1 $M_\odot$. While this mass is only 0.3 $M_\odot$ lower than what current observations with Hubble can achieve, it should be emphasised that this increase of "only" 0.3 $M_\odot$ will reveal the majority of M-type stars, which account for almost three quarters of all main sequence stars (Ledrew 2001). Given that the limit of current studies is around the 0.5 $M_\odot$ knee from Kroupa (2001), opening up this range will allow future studies to pin down exactly what the shape of the IMF looks like in the LMC clusters.

As previously noted the exposure time for the simulated images was one hour. By observing for longer times, the lowest observable mass will decrease, however the change is disproportionate to the exposure time. Leschinski et al. (2016) show that increasing the exposure time to 10 hours per cluster only increases the sensitivity limit by around 1.5^m and 1^m in the J and K_S filters respectively. For the case of the LMC, this would decrease the lowest observable mass to around 0.06$M_\odot$, i.e. just below the hydrogen burning limit.

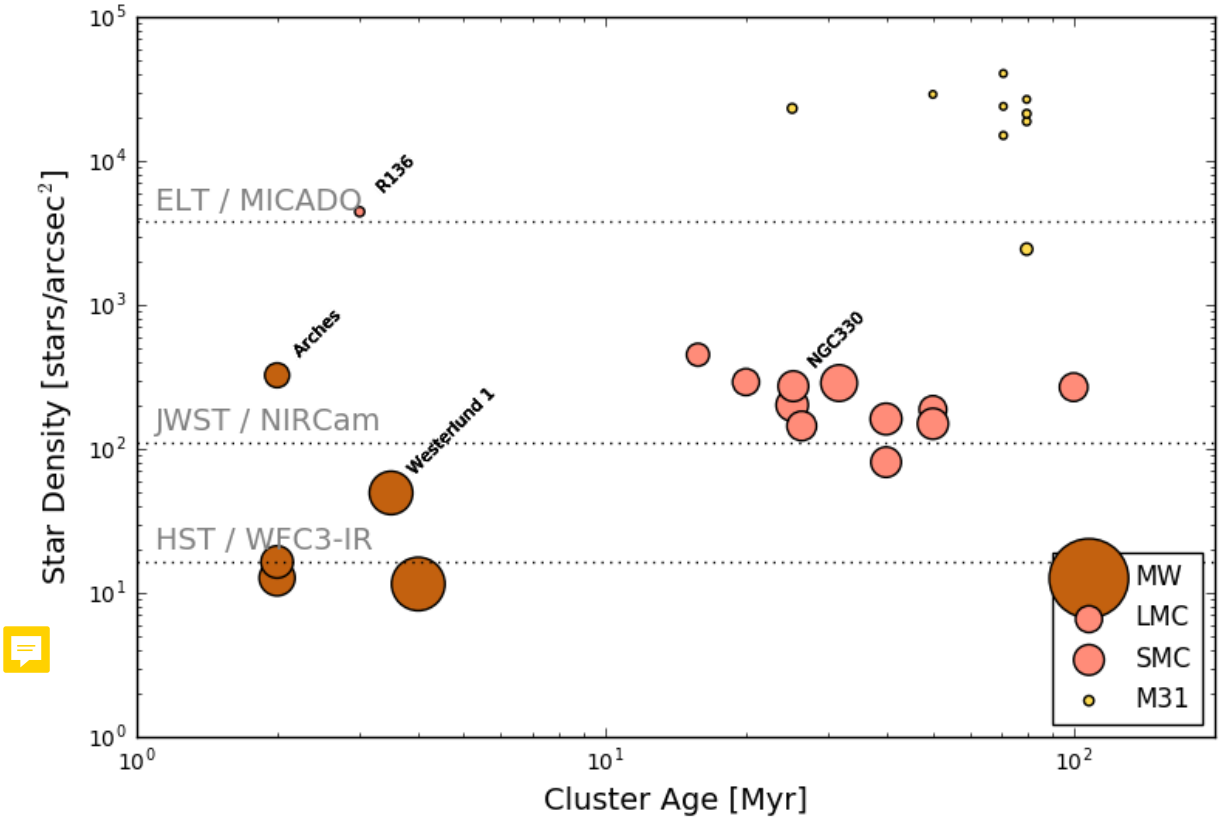

Fig. 3. The stellar densities in the cores of the clusters listed in Table A.1 assuming a sensitivity limit of K_S=28^m . The size of the circles is proportional (including an offset) to the relative on-sky size of the cluster cores. The colours reflect the lowest possible reliably observable mass, as shown in Figure 2 and listed in Table A.1. Brown: M>0.01$M_\odot$; Pink: M>0.1$M_\odot$; Yellow: M>0.9$M_\odot$. The densities shown here take into account the sensitivity limit and therefore are only for the potentially observable stars, i.e. any low luminosity stars with K_S>28^m are omitted from the density calculation. This is equivalent to all stars in the Milky Way, M-class stars and brighter in the LMC, and G-class stars and brighter in M31. Only clusters from Portegies Zwart et al. (2010) which have a defined core radius, r_c, are shown. The dashed lines in this figure represent the (estimated) limit to the resolving capability of the HST, JWST and ELT. We define the limiting density as the mean distance between stars being equal to 2.5× the PSF FWHM. Given the predicted PSF shapes for the latter two telescopes, these lines may prove to be somewhat optimistic. Nevertheless the graphic illustrates the point that cores of the majority of young clusters outside the Milky Way are far too dense for either HST or JWST observations. Thus it will require the ELT (or similar) to study the most heavily populated regions of these clusters.

It should be noted that the majority of young clusters have cores less dense than that of Westerlund 1, and therefore the limiting observable mass will also be lower than the 0.5 $M_\odot$ mass quoted for a Westerlund 1-like YMC in the LMC. Given MICADO's resolving power it will therefore also be possible to determine to what extent apparent mass segregation has played a role in previous studies of the IMF in the LMC. More to the point MICADO will enable us to understand the apparent deviations from the Salpeter IMF as reported by Da Rio et al. (2009), Geha et al. (2013) and Kalirai et al. (2013).

At distances of 100 kpc to 200 kpc and with careful photometry and longer observations MICADO should be able to detect stars down to the sensitivity limit of 0.5 $M_\odot$. This will only be possible though for clusters with stellar densities less than 10^4 stars arcsec^{-2} . As a reference an ONC-like cluster at a distance of 200 kpc will have a stellar density on the order of 10^5 stars arcsec^{-2} . Such observations will be useful for determining the composition of OB associations and sparser (older) open clusters, if there were any present in the non-Magellanic satellites of the Milky Way. Nevertheless MICADO will still allow us observe the fabled 0.5 $M_\odot$ knee in the field population of the nearest low metallicity dwarf spheroidal galaxies.

Closer to home MICADO should be able detect 10 M_{Jup} objects in an ONC-like clusters at a distance of 8 kpc. The Arches cluster is an obvious candidate for such studies, and given its proximity to the galactic centre makes it an ideal case to study the IMF under extreme conditions. The main hindrance to such observations is not the almost 2 mag of variable Ks-band extinction along the line of site (Espinoza et al. 2009), but rather the brightest stars in the cluster. The effectiveness of MICADO observations will also be limited by the brightest stars in the field. Leschinski (2018, in prep) state that point sources with magnitudes K_S>14.8^m will saturate the MICADO detectors within the 2.6 s minimum exposure time. There are very few regions in the cores of Milky Way open clusters which do not contain stars brighter than K_S ~15^m , making deep MICADO observations of these regions difficult.

3.2. The core densities of young star clusters

The second of the questions we asked with this study was "What instrumental effects will play a critical role when undertaking such studies with MICADO and the ELT?". The instrumental effect which would play the largest role regarding the accuracy of the estimates given here is our knowledge of the PSF. For this study we used a single SCAO PSF. We assumed that the PSF orientation stayed the same for the length of the observation. Consequently we had a very good model of our reference star for the PSF subtraction. This will obviously not be the case for real observations as the pupil of the telescope will rotate with respect to the sky, causing an axial broadening of the PSF over the course of an observing run. On the one hand this broadening should improve the results from our subtraction method as it will smooth out many of the sharp features of the instantaneous PSF. On the other hand we will lose information on both the structure of the PSF and the extent of the wings. Thus the PSF subtraction algorithm will less accurately be able to estimate the background level when fitting the reference PSF to a star. As a consequence faint stars caught in the PSF wings of the brighter stars may not be detected as often as they would be if the PSF remained rotationally aligned with the sky. A hybrid approach to the faint star subtraction problem may be the following: Subtract the brightest stars from each individual exposure using an instantaneous PSF derived from the brightest stars in that exposure, then stack the residual images and extract the faintest stars using a rotationally broadened PSF. Further investigation is required to determine whether this approach would indeed increase the detection rate for faint stars.

Although it may seem obvious, it is worth mentioning that it is clear from our simulations that resolving stellar densities of 10^3 stars arcsec^{-2} is well within the capabilities of MICADO. With an optimised PSF fitting and subtraction algorithm, extracting upwards of $5{\times}10^3$ stars arcsec^{-2} should also be in the realms of possibility. $5{\times}10^3$ stars arcsec^{-2} is equivalent to approximately one star in an area equivalent to ~2.5 ELT H-band PSF FWHMs. This is similar to being able to resolve every star in the core of an ONC-like cluster in the LMC. For JWST and HST the equivalent stellar densities are only 160 stars arcsec^{-2} and 20 stars arcsec^{-2} respectively. Although MICADO may not have the sensitivity of a space-based telescope, the resolving power will give us full access to the core populations of dense stellar clusters in the major satellites of the Milky Way.

3.3. Opportunities and targets for future observations with MICADO and the ELT

These simulations are a nice theoretical exercise, however without an application to observations they are not all that useful. Figure 3 shows the estimated stellar densities in the cores of the open clusters and YMCs compiled by Portegies Zwart et al. (2010). The density values, $\log_{10}(\rho)$, only take into account the stars with apparent magnitudes above the sensitivity limit of MICADO and thus reflect the "real" observable density for the clusters (Also listed in Table A.1). The limits set for HST, JWST and MICADO are the critical stellar density above which our extraction algorithm struggles to detect and remove more than 90% of the stars in a field. We find that for the Galactic clusters, the resolution of JWST will be sufficient to resolve all stars in most cluster cores down to the sensitivity limit of the instrument.

For clusters in the galactic plane though JWST observations will struggle to disentangle the cluster stars from the field stars. To robustly determine cluster membership, observations of the proper motion of the cluster relative to the field will be required. Stolte et al. (2008) show that the proper motion of the Arches cluster near the Galactic centre is ~5 mas yr^{-1}. This equates to around a sixth the size of a pixel in the JWST NIRCam instrument. MICADO, in contrast, will have a plate scale of 1.5 mas in the high resolution mode, meaning that cluster membership could be determined by observations spaced only several months apart.

Further afield, resolving the cores of the massive young clusters in the Magellanic clouds will not be possible with JWST. MICADO however will enable access to these cluster cores, which in turn will open up to possibility to study the dynamical processes (e.g. evaporation, core collapse, etc.) involved in the evolution of extra-galactic clusters. Additionally observations of a series of LMC clusters with varying ages will give a much better picture of how the initial mass function evolves into the present day mass function, and how the dynamical evolution of the cluster influences the observations, and calculations of, a cluster's IMF.

Portegies Zwart et al. (2010) provides a curated list of the most well known massive young clusters in- and outside the Milky Way. However many more clusters exist within the local group of galaxies. Indeed to fully understand the environmental dependence on cluster formation and evolution, a statistically large number of extra-galactic cluster will need to be observed. Figure 4 shows the pool of clusters available to MICADO at the ELT along with the corresponding observational limits of stars of various masses. The blue curve in Figure 4 shows the cumulative number of possible MICADO targets reported in catalogues and the literature for both the Milky Way and in galaxies out to 2 Mpc (for references see Table A.2). The red dotted curve adds the approximate number of additional clusters in the local group which have not yet been catalogued. This estimate is based on each galaxy's total H_α flux with the conversion to approximate number of clusters based on the H_α derived star formation rate and young cluster catalogue for M31 (See (**?**)).

What is evident from Figure 4 is that there exist hundreds (potentially thousands) of clusters within a 2 Mpc radius that will be observable by MICADO, which could be used for a statistical analysis of the IMF under varying environmental conditions.

What more can we say here??

4. Conclusion

MICADO and the ELT will provide the chance to finally resolve the core populations of the densest star clusters in the Milky Way and in neighbouring galaxies out to distances of a several hundred kiloparsecs. By turning MICADO towards young stellar clusters we hope to finally answer the question as to whether the IMF distribution is indeed universal, or whether its shape changes when we leave the solar neighbourhood. Currently these answers are locked up inside the dense cores of young stellar clusters. Observations of these clusters are primarily limited by confusion. Determining exactly how much more of these stellar populations will be visible to MICADO was the primary goal of this work.

This study aimed to answer two questions: What is the lowest mass star that MICADO will be able to observe reliably for a given stellar density and distance? And what instrumental effects will play a critical role when undertaking such studies with MICADO and the ELT? In order to answer these we used the instrument simulator for MICADO (SimCADO) to generate "observations" of 42 dense stellar regions corresponding to the cores

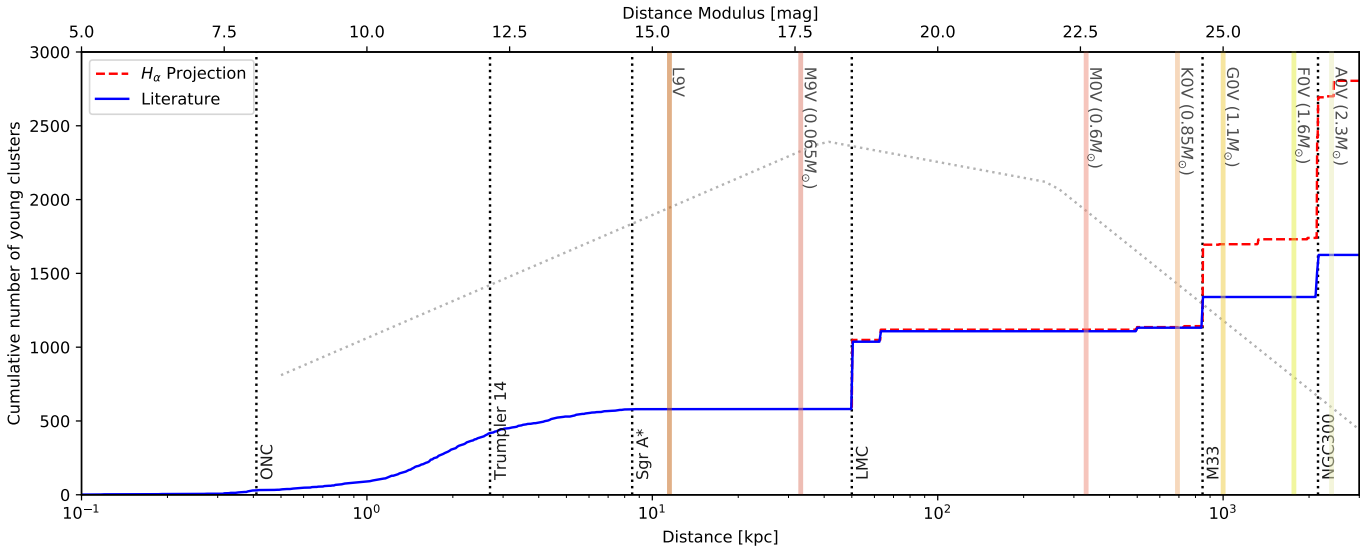

Fig. 4. The blue line show the cumulative number of young clusters with increasing distance from Earth as reported in catalogues and the literature. The red dotted line shows the expected number of young clusters in a given galaxy based on an extrapolation of the galaxy's star formation rate from its total H_α flux. The solid vertical lines represent the observational horizons for given stellar spectral types assuming a detection limit of K=28^m with MICADO at the ELT. The faint dotted grey line shows the corresponding approximation distance limits for determining the slope of various regions of the IMF using MICADO. The population of Milky Way clusters is taken from the HEASARC Milky Way Open Cluster database (MWOCDB, **?**) as represents only the clusters located at declinations accessible to MICADO (-85° < δ < +35°)

of young stellar clusters at varying distances from earth. Here we present a brief summary of the results:

- We have shown that MICADO will easily be able to resolve all members of a stellar population with a density up to 10^3 stars arcsec^{-2} . With proper knowledge of the PSF and an optimised detection and subtraction algorithm densities of $5{\times}10^3$ stars arcsec^{-2} should also be achievable.
- Given that MICADO observations will be constrained by the instrument's sensitivity to both the brightest and faintest sources in the field of view, MICADO is best suited to investigate the shape of the IMF in clusters in the outer edges of the Milky Way as well as the nearest galaxies. For real world science cases this means that the cores of dense young star clusters such as R136 in the LMC and NGC330 in the SMC will be resolvable with MICADO.
- Observations focusing on the initial mass function of clusters in the LMC will be limited by sensitivity, not crowding, to 0.1 $M_\odot$. This means that investigations of the brown dwarf knee (~0.08 $M_\odot$) will not be possible outside the Milky Way, however MICADO's resolution will allow the peak of the IMF (0.1 $M_\odot$ <M <0.5 $M_\odot$) to be extensively investigated in the Magellanic clouds, and the high mass function out to distances of 5 Mpc.
- Comparison of logNormal vs broken power law
- The brown dwarf population will be accessible in the cores of the densest Milky Way clusters, e.g. in the Arches and Westerlund clusters. Objects with masses on the order of 10 M_{Jup} will be accessible by MICADO for clusters within 8 kpc of Earth. The only caveat is that an appropriate observation strategy must be found to mask the many bright ($m_{Ks} < 15^m$) stars in these clusters.
- Finally accurate knowledge of the ELT's PSF will be absolutely essential for good photometry and PSF subtraction algorithms. The sharp structures created by the segmented mirror design lead to many fake low luminosity star detections if either the PSF is not well known or the extraction algorithm is not capable of differentiating between a star and an artefact of the PSF.

Acknowledgements. KL would also like to express his gratitude to Gijs Verdoes Kleijn, Eline Tolstoy, and Ric Davies for the insightful and helpful comments and discussions regarding future possible observations with the ELT. SimCADO incorporates Bernhard Rauscher's HxRG Noise Generator package for python (Rauscher 2015). This research made use of POPPY, an open-source optical propagation Python package originally developed for the James Webb Space Telescope project (Perrin et al. 2015). This research made use of Astropy, a community-developed core Python package for astronomy (Astropy Collaboration et al. 2013; The Astropy Collaboration et al. 2018). This research made use of Photutils (Bradley et al. 2017). This research has made use of "Aladin sky atlas" developed at CDS, Strasbourg Observatory, France (Bonnarel et al. 2000; Boch & Fernique 2014). SimCADO makes use of atmospheric transmission and emission curves generated by ESO's SkyCalc service, which was developed at the University of Innsbruck as part of an Austrian in-kind contribution to ESO. This research is partially funded by the project IS538003 of the Hochschulraumstrukturmittel (HRSM) provided by the Austrian Government and administered by the University of Vienna.

References

Astropy Collaboration, Robitaille, T. P., Tollerud, E. J., et al. 2013, A&A, 558, A33
Bastian, N., Covey, K. R., & Meyer, M. R. 2010, Annu. Rev. Astron. Astrophys., 48, 339
Boch, T. & Fernique, P. 2014, in Astronomical Society of the Pacific Conference Series, Vol. 485, Astronomical Data Analysis Software and Systems XXIII, ed. N. Manset & P. Forshay, 277
Bonnarel, F., Fernique, P., Bienaymé, O., et al. 2000, A&AS, 143, 33
Bradley, L., Sipocz, B., Robitaille, T., et al. 2017, astropy/photutils: v0.4
Chabrier, G. 2005, in Astrophysics and Space Science Library, Vol. 327, The Initial Mass Function 50 Years Later, ed. E. Corbelli, F. Palla, & H. Zinnecker, 41
Clénet, Y., Buey, T., Rousset, G., et al. 2016, in Proc. SPIE, Vol. 9909, Society of Photo-Optical Instrumentation Engineers (SPIE) Conference Series, 99090A
Da Rio, N., Gouliermis, D. A., & Henning, T. 2009, ApJ, 696, 528
Davies, R., Ageorges, N., Barl, L., et al. 2010, in Proc. SPIE, Vol. 7735, Ground-based and Airborne Instrumentation for Astronomy III, 77352A

Davies, R., Schubert, J., Hartl, M., et al. 2016, in Proc. SPIE, Vol. 9908, Society of Photo-Optical Instrumentation Engineers (SPIE) Conference Series, 99081Z
Diolaiti, E. 2010, The Messenger, 140, 28
Espinoza, P., Selman, F. J., & Melnick, J. 2009, A&A, 501, 563
Gallart, C., Freedman, W. L., Aparicio, A., Bertelli, G., & Chiosi, C. 1999, AJ, 118, 2245
Geha, M., Brown, T. M., Tumlinson, J., et al. 2013, ApJ, 771, 29
Gilmozzi, R. & Spyromilio, J. 2007, The Messenger, 127
Kalirai, J. S., Anderson, J., Dotter, A., et al. 2013, ApJ, 763, 110
Kroupa, P. 2001, MNRAS, 322, 231
Kroupa, P. 2002, Science, 295, 82
Ledrew, G. 2001, JRASC, 95, 32
Leschinski, K., Czoske, O., Köhler, R., et al. 2016, in Proc. SPIE, Vol. 9911, Society of Photo-Optical Instrumentation Engineers (SPIE) Conference Series, 991124
Lim, B., Chun, M.-Y., Sung, H., et al. 2013, AJ, 145, 46
Mel'Nik, A. M. & Efremov, Y. N. 1995, Astronomy Letters, 21, 10
Pecaut, M. J. & Mamajek, E. E. 2013, ApJS, 208, 9
Perrin, M. D., Long, J., Sivaramakrishnan, A., et al. 2015, WebbPSF: James Webb Space Telescope PSF Simulation Tool, Astrophysics Source Code Library
Piskunov, A. E., Schilbach, E., Kharchenko, N. V., Röser, S., & Scholz, R.-D. 2007, A&A, 468, 151
Portegies Zwart, S. F., McMillan, S. L. W., & Gieles, M. 2010, ARA&A, 48, 431
Rajan, A. & et al. 2011, WFC3 Data Handbook v. 2.1 (STSci)
Rauscher, B. J. 2015, PASP, 127, 1144
Salpeter, E. E. 1955, ApJ, 121, 161
Sirianni, M., Nota, A., Leitherer, C., De Marchi, G., & Clampin, M. 2000, ApJ, 533, 203
Stolte, A., Ghez, A. M., Morris, M., et al. 2008, ApJ, 675, 1278
The Astropy Collaboration, Price-Whelan, A. M., Sipőcz, B. M., et al. 2018, ArXiv e-prints [arXiv:1801.02634]

Table .1. The age and observable stellar densities for a selection of young massive clusters found both in and outside the Milky Way, as listed in Portegies Zwart et al. (2010). The densities have been calculated to only include stars which are brighter than Ks=28^{m} , as fainter stars will not be detectable by MICADO. The table list the parameters for the clusters shown in Fig. 3.

Galaxy	Cluster	Distance kpc	Age Myr	log(Mass) $M_\odot$	Core radius arcsec	$\log_{10}(\rho)$ stars arcsec^{-2}	Limiting mass $M_\odot$
Cores resolvable by HST							
MW	ONC	0.4	1	3.7	100	-1.6	0.01
Cores resolvable by JWST							
MW	Trumpler-14	2.7	2	4	10.7	1.1	0.01
MW	Quintuplet	8.5	4	4.0	24	1.1	0.04
MW	NGC3603	3.6	2	4.1	8.6	1.2	0.01
MW	Westerlund-1	5.2	3.5	4.5	15.9	1.7	0.01
LMC	NGC2214	50	39.8	4.0	7.5	1.9	0.1
Cores resolvable by MICADO							
LMC	NGC1847	50	26.3	4.4	7.1	2.2	0.1
LMC	NGC2157	50	39.8	4.3	8.2	2.2	0.1
LMC	NGC1711	50	50.1	4.2	7.9	2.2	0.1
LMC	NGC1818	50	25.1	4.4	8.5	2.3	0.1
LMC	NGC2164	50	50.1	4.2	6.1	2.3	0.1
SMC	NGC330	63	25.1	4.6	7.7	2.4	0.15
LMC	NGC2136	50	100	4.3	6.6	2.4	0.1
MW	Arches	8.5	2	4.3	4.9	2.5	0.04
LMC	NGC1850	50	31.6	4.9	11	2.5	0.1
LMC	NGC2004	50	20	4.4	5.8	2.5	0.1
LMC	NGC2100	50	15.8	4.4	4.1	2.7	0.1
M31	B257D	780	79.4	4.5	0.8	3.4	0.9
Only outer regions resolvable by MICADO							
LMC	R136	50	3	4.8	0.41	3.7	0.1
M31	B066	780	70.8	4.3	0.10	4.2	0.9
M31	B040	780	79.4	4.5	0.15	4.3	0.9
M31	B043	780	79.4	4.4	0.19	4.3	0.9
M31	B318	780	70.8	4.4	0.05	4.4	0.9
M31	B448	780	79.4	4.4	0.05	4.4	0.9
M31	Vdb0	780	25.1	4.9	0.37	4.4	0.9
M31	B327	780	50.1	4.4	0.05	4.5	0.9
M31	B015D	780	70.8	4.8	0.06	4.6	0.9

Table .2. References for the cumulative cluster numbers within a 2 Mpc radius which will be observable by MICADO at the ELT. Star formation rate estimates are based on the integrated galaxy H_α fluxes from **?** and were used to estimate the true number of open clusters contained in each galaxy. The Milky Way clusters were taken from the HEASARC Milky Way Star Cluster catalogue (**?**) and filtered to only include clusters visible to MICADO at the ELT (i.e. Dec < +35 deg).

Name	SFR [$M_\odot$ / yr]	Distance [kpc]	N Clusters	Reference
MilkyWay		8	590	Kharchenko+13
LMC	0.30	50	456	Glatt+10
SMC	0.05	63	71	Glatt+10
NGC6822	0.01	499	24	Karampelas+09
M33	0.36	847	208	Fan+14
NGC0055	0.45	2128	168	Castro+08
NGC0300	0.18	2148	117	Pietrzynski+01
NGC4214	0.15	2938	52	Andrews+13

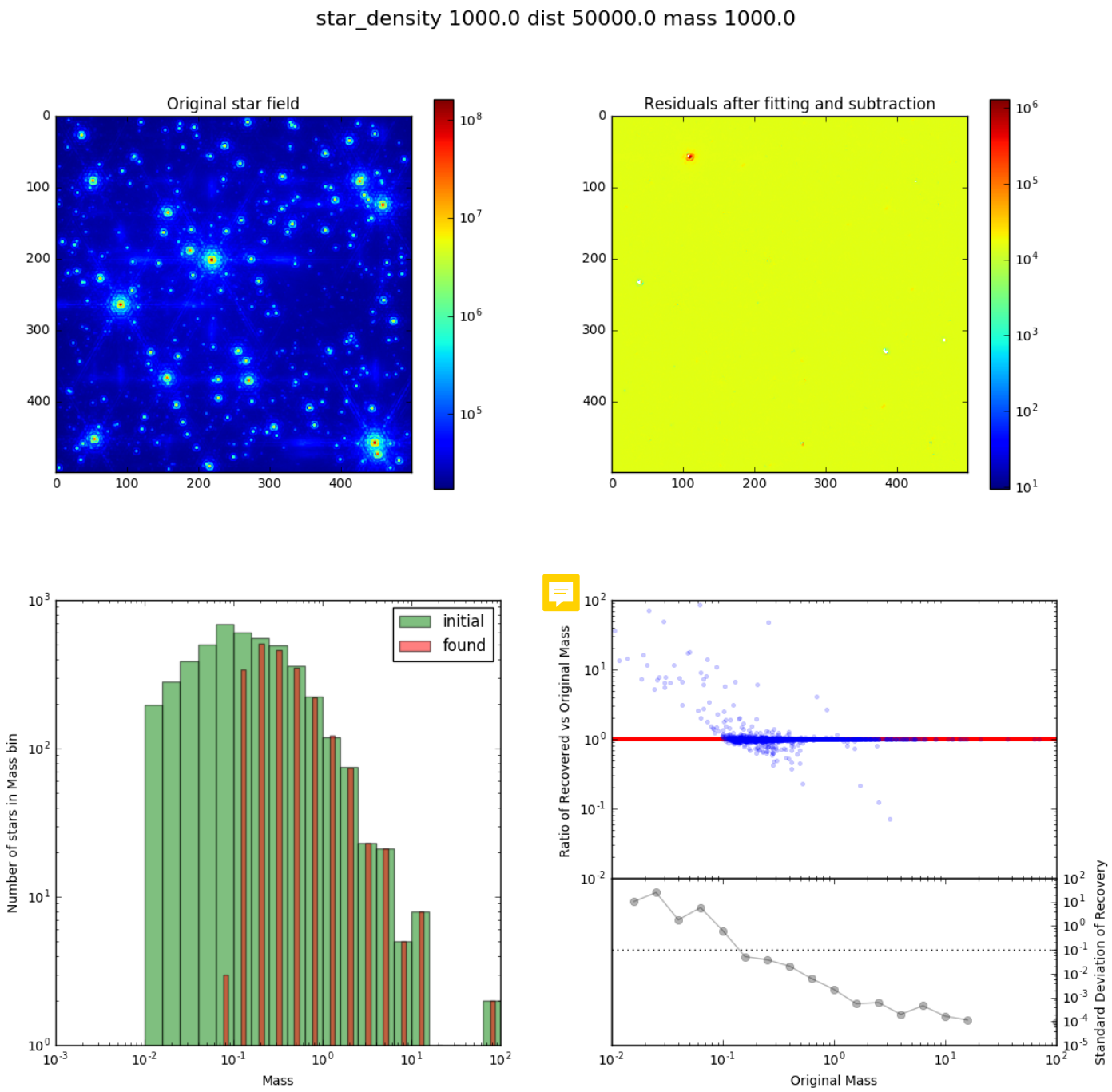

Fig. .1. Results of extracting stars from a 1000 stars arcsec^{-2} cluster at a distance of 50 kpc. Top left: The original 2"×2" stellar field with a density of 10^3 stars arcsec^{-2} . The stars in the field have masses between 0.01 $M_\odot$ and 300 $M_\odot$. The PSF used in this study was an instantaneous SCAO PSF, similar to what would be seen on a single MICADO detector 2.6 s exposure. Top right: The same field after our detection and subtraction algorithm has iteratively removed all the stars. 10^3 stars arcsec^{-2} are extracted reasonably easily by our algorithm. Bottom left: The fraction of extracted stars in each mass bin which matched up with the original list of stars. The majority of stars more massive than 0.1 $M_\odot$ were detected. Bottom right: The upper panel shows the ratio of extracted mass to original mass. The vast majority of the almost 4000 stars in the image fell almost perfectly on the red one-to-one line. The minor scatter around the line is due to a combination of our detection algorithm not being able to discern between to very close stars, and contamination for the PSF artefacts, e.g. the segmented diffraction spikes. The lower panel shows the standard deviation of masses around the one-to-one line in a certain mass bin. A mass bin was deemed reliable if the average recovered to original mass ratio was in the range 1±0.1 and the standard deviation was less than 10%.

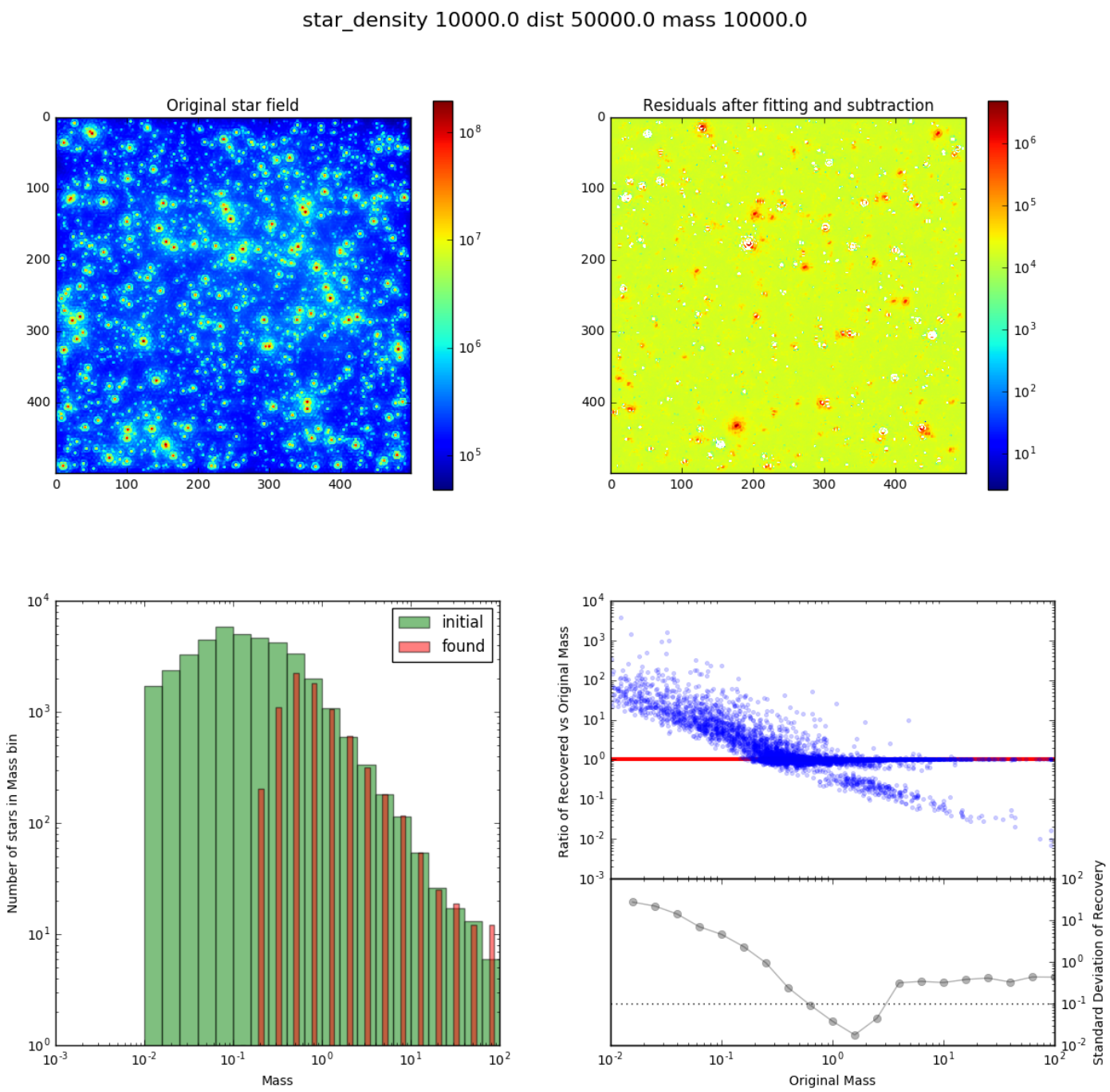

Fig. .2. Same as Fig. A.1 but for a stellar density of 10^4 stars arcsec^{-2} . At these densities the number of "double" stars has increased to the point where our detection algorithm was unable to accurately fit and subtract the a number of the bright stars. Although a large number of incorrect mass determinations are visible in the big blue cloud, still around 60% of the ~40 000 sources in this image fall on the red one-to-one line. The segmented PSF meant that the the algorithm detected many fake sources which skewed the detection statistics in both the high and low mass regimes. We are still looking into ways of preventing this from happening in future studies.